RIMS Kôkyûroku Bessatsu
B60 (2016), 15–32

Multiwavelet analysis and its application to signal processing

By

Ryuichi Ashino*

Abstract

It is important to use several wavelet functions having different characteristics and to compare their continuous wavelet transforms. To explain such procedure in the unified way, the notion of the continuous multiwavelet transform and its essentials are introduced. An application to blind signal separation is presented.

This article is a survey, without proofs, of some results of collaborated research with Takeshi Mandai, Osaka Electro-Communication University, Japan and Akira Morimoto, Osaka Kyoiku University, Japan.

§ 1. Fundamental unitary operators in time-frequency analysis

Let us define three fundamental unitary operators in time-frequency analysis. Denote by $\mathcal{T}_b$ the *translation* operator by $b \in \mathbb{R}^n$:

$$(\mathcal{T}_b f)(x) = f(x-b),$$

by $\mathcal{M}_\omega$ the *modulation* operator by $\omega \in \mathbb{R}^n$:

$$(\mathcal{M}_\omega f)(x) = e^{i\omega\cdot x} f(x),$$

by $\mathcal{D}_a$ the *dilation* operator by $a \in \mathbb{R}_+ := \{x \in \mathbb{R} \mid x > 0\}$:

$$(\mathcal{D}_a f)(x) = a^{-n/2} f(x/a).$$

Received October 9, 2015. Revised May 31, 2016.
2010 Mathematics Subject Classification(s): Primary: 42C40; Secondary: 94A12, 65T60
Key Words: *blind signal source separation, continuous multiwavelet transform, time-frequency analysis.*
Supported by JSPS.KAKENHI(C)25400202 of Japan.
*Mathematical Sciences, Osaka Kyoiku University, Osaka 582-8582, Japan.
e-mail: ashino@cc.osaka-kyoiku.ac.jp

These three operators, $\mathcal{T}_b$, $\mathcal{M}_\omega$, $\mathcal{D}_a$, are unitary on $L^2(\mathbb{R}^n)$, hence their adjoints are given by their inverses:

$$\mathcal{T}_b^* = \mathcal{T}_{-b}, \qquad \mathcal{M}_\omega^* = \mathcal{M}_{-\omega}, \qquad \mathcal{D}_a^* = \mathcal{D}_{1/a}.$$

Lemma 1.1 (Commutation relation)**.**

$$\begin{aligned} \mathcal{T}_y\mathcal{M}_\xi &= e^{-i\xi y}\mathcal{M}_\xi\mathcal{T}_y, & \mathcal{M}_\xi\mathcal{T}_y &= e^{i\xi y}\mathcal{T}_y\mathcal{M}_\xi, \\ \mathcal{T}_y\mathcal{D}_\rho &= \mathcal{D}_\rho\mathcal{T}_{y/\rho}, & \mathcal{D}_\rho\mathcal{T}_y &= \mathcal{T}_{\rho y}\mathcal{D}_\rho, \\ \mathcal{M}_\xi\mathcal{D}_\rho &= \mathcal{D}_\rho\mathcal{M}_{\rho\xi}, & \mathcal{D}_\rho\mathcal{M}_\xi &= \mathcal{M}_{\xi/\rho}\mathcal{D}_\rho. \end{aligned}$$

Define the Fourier transform of a function $f \in L^1(\mathbb{R}^n)$ and the inverse Fourier transform of a function $g \in L^1(\mathbb{R}^n)$ by

$$\begin{aligned} \mathcal{F}(f)(\xi) = \widehat{f}(\xi) &:= \int_{\mathbb{R}^n} e^{-ix\cdot\xi}\, f(x)\, dx, \\ \mathcal{F}^{-1}(g)(x) = \check{g}(x) &:= (2\pi)^{-n} \int_{\mathbb{R}^n} e^{ix\cdot\xi}\, g(\xi)\, d\xi, \end{aligned}$$

where $i = \sqrt{-1}$.

Lemma 1.2 (Commutation relation with Fourier transform)**.**

$$\mathcal{F}[\mathcal{T}_y f] = \mathcal{M}_{-y}\mathcal{F}[f], \qquad \mathcal{F}[\mathcal{M}_\omega f] = \mathcal{T}_\omega\mathcal{F}[f], \qquad \mathcal{F}[\mathcal{D}_\rho f] = \mathcal{D}_{1/\rho}\mathcal{F}[f].$$

As the dilation $\mathcal{D}_a$ and the translation $\mathcal{T}_b$ are unitary, their composition $\mathcal{T}_b\mathcal{D}_a$ is also unitary and called *time-scale operator*.

Lemma 1.3 (Composition of time-scale operators)**.**

$$(\mathcal{T}_b\mathcal{D}_a)(\mathcal{T}_t\mathcal{D}_s) = \mathcal{T}_{at+b}\mathcal{D}_{as}, \qquad b, t \in \mathbb{R}^n, \quad a, s \in \mathbb{R}_+.$$

§ 2. Center and width of a window function

Let us denote by $(f, g) := \displaystyle\int_{\mathbb{R}^n} f(x)\overline{g(x)}\, dx$ the canonical inner product of $L^2(\mathbb{R}^n)$ and by $\|f\| := \sqrt{(f, f)}$ the canonical norm. To investigate properties of a given function $f(x)$, we often represent $f(x)$ as a superposition of well-known functions $g_j(x)$ or $g(s, x)$, $s \in \Omega$, such that $f(x) = \sum_j a_j g_j(x)$ or $f(x) = \displaystyle\int_\Omega a(s)g(s, x)\, ds$. The Fourier inversion formula:

$$f(x) = (2\pi)^{-n} \int_{\mathbb{R}^n} e^{ix\cdot\xi}\, \widehat{f}(\xi)\, d\xi$$

can be regarded as one of such representations. But the functions $e^{ix\cdot\xi}$ are not localized in space. Therefore, the *windowed Fourier transform*:

$$\begin{aligned} V_w f(b,\omega) &:= \big(f(x), e^{ix\cdot\omega} w(x-b)\big) \\ &= (f, \mathcal{M}_\omega \mathcal{T}_b w) \end{aligned}$$

was proposed to access the local information both in space and in frequency. In fact, Parseval's formula and the commutation relations $\mathcal{F}\mathcal{M}_\omega = \mathcal{T}_\omega \mathcal{F}$, $\mathcal{F}\mathcal{T}_b = \mathcal{M}_{-b}\mathcal{F}$ imply

$$\begin{aligned} (f, \mathcal{M}_\omega \mathcal{T}_b w) &= (2\pi)^{-n} \left(\mathcal{F}f, \mathcal{F}\mathcal{M}_\omega \mathcal{T}_b w\right) \\ &= (2\pi)^{-n} \left(\widehat{f}, \mathcal{T}_\omega \mathcal{M}_{-b} \widehat{w}\right) \\ &= (2\pi)^{-n} e^{-i\omega\cdot b} \left(\widehat{f}, \mathcal{M}_{-b} \mathcal{T}_\omega \widehat{w}\right). \end{aligned}$$

Hence, $V_w f(b,\omega)$ can access the information on both areas localized by $w(x-b)$ in space and by $\widehat{w}(\xi-\omega)$ in frequency.

For a function $w \in L^2(\mathbb{R}^n)$, the *center* c_w of w is defined by

$$\begin{aligned} c_w &= (c_{w,1}, \ldots, c_{w,n}), \\ c_{w,j} &:= \frac{1}{||w||^2} \int_{\mathbb{R}^n} x_j |w(x)|^2 \, dx, \quad j = 1, \ldots, n, \end{aligned}$$

and the *width* Δ_w of w is defined by

$$\begin{aligned} \Delta_w &:= (\Delta_{w,1}, \ldots, \Delta_{w,n}), \\ \Delta_{w,j} &:= \frac{1}{||w||} \left(\int_{\mathbb{R}^n} (x_j - c_{w,j})^2 |w(x)|^2 \, dx \right)^{1/2}. \end{aligned}$$

Denote by $|\cdot|$ the length of a vector. A function $w \in L^2(\mathbb{R}^n) \setminus \{0\}$ is called a *window function* if $|x|w(x) \in L^2(\mathbb{R}^n)$, for which we can define c_w and Δ_w. Hereafter, we assume that both w and its Fourier transform $\widehat{w}$ are window functions. Let us denote $x^* = (x_1^*, \ldots, x_n^*)$ and $\xi^* = (\xi_j^*, \ldots, \xi_n^*)$ the centers of w and $\widehat{w}$, respectively. We also denote $\Delta_w = (\Delta_{w,1}, \ldots, \Delta_{w,n})$ and $\Delta_{\widehat{w}} = (\Delta_{\widehat{w},1}, \ldots, \Delta_{\widehat{w},n})$ the widths of w and $\widehat{w}$, respectively. Then, as an analogue of the one dimensional uncertainty principle in Fourier analysis, we have

$$\Delta_{w,j} \Delta_{\widehat{w},j} \geq \frac{1}{2}, \qquad j = 1, \ldots, n,$$

which shows that the localization is a trade-off between w and $\widehat{w}$. We also have

$$|\Delta_w| \, |\Delta_{\widehat{w}}| \geq \frac{n}{2}.$$

The rectangular parallelepiped defined by

$$\prod_{j=1}^{n} [x_j^* - \Delta_{w,j}, x_j^* + \Delta_{w,j}] \times [\xi_j^* - \Delta_{\widehat{w},j}\,, \xi_j^* + \Delta_{\widehat{w},j}\,]$$

is called the *time-frequency window* of $w(x)$, whose projection to the (x_j, ξ_j)-plane is illustrated in Figure 1.

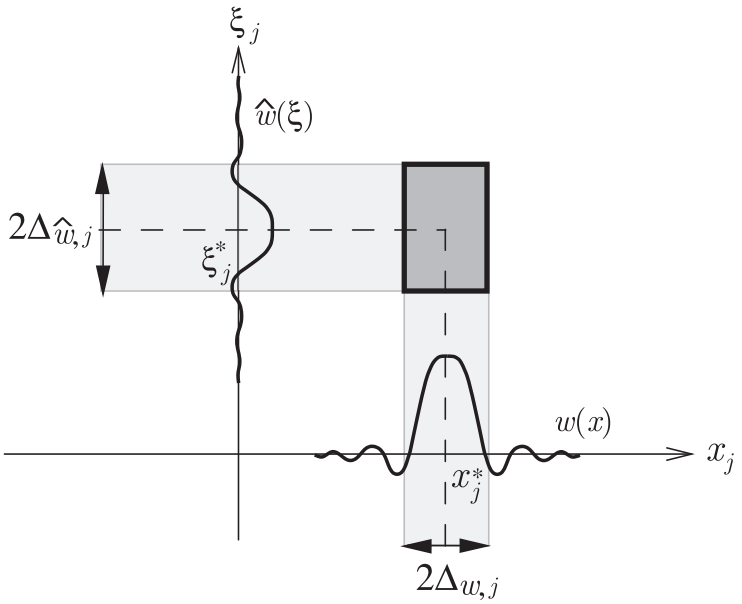

Figure 1. The projection of the time-frequency window of $w(x)$ to the (x_j, ξ_j)-plane.

§ 3. Continuous wavelet transform

Wavelet analysis can be used as a tool for time-frequency analysis. The continuous wavelet transform correlates a given function $f \in L^2(\mathbb{R}^n)$ with a family of waveforms $\{\mathcal{T}_b \mathcal{D}_a \psi\}$, where $\psi \in L^2(\mathbb{R}^n)$ is called a *wavelet function*. If the wavelet function ψ is properly chosen so as to be concentrated in "time" x and in "frequency" ξ, the continuous wavelet transform of f can be regarded as a time-frequency information of f. One advantage of the continuous wavelet transform is variety of wavelet functions. Each wavelet function has its own unique characteristics.

Definition 3.1. The *continuous wavelet transform* of $f \in L^2(\mathbb{R}^n)$ with respect to a wavelet function $\psi \in L^2(\mathbb{R}^n)$ is defined by

$$\begin{aligned}(W_\psi f)(b,a) :=& (f, \mathcal{T}_b \mathcal{D}_a \psi) \\ =& (2\pi)^{-n} \left(\widehat{f}, \mathcal{M}_{-b} \mathcal{D}_{1/a} \widehat{\psi}\right), \quad a \in \mathbb{R}_+,\ b \in \mathbb{R}^n.\end{aligned}$$

Theorem 3.2 (Inversion formula). *Assume $\psi \in L^2(\mathbb{R}^n)$ satisfies the following admissibility condition: there exists a positive constant K such that*

$$\int_{\mathbb{R}_+} |\widehat{\psi}(a\omega)|^2 \frac{da}{a} = K, \qquad \text{for almost all } \omega \in S^{n-1},$$

where S^{n-1} is the unit sphere in $\mathbb{R}^n$. Then,

$$f = \frac{1}{K} \int_{\mathbb{R}^n} \int_{\mathbb{R}_+} (W_\psi f)(b,a) \mathcal{T}_b \mathcal{D}_a \psi \frac{db\, da}{a^{n+1}}, \qquad f \in L^2(\mathbb{R}^n).$$

§ 4. One-dimensional continuous wavelet transform

To clarify our problems, let us start with one dimensional continuous wavelet transform. We use the wavelet toolbox in MATLAB. The wavelet toolbox provides a data, named cuspamax, f for demonstration which is illustrated in Figure 2, the top-left. Since $(W_\psi f)(b,a)$ is two-dimensional data, we need a visual method of displaying the wavelet transform. Usually we use the intensity image, called *scaleogram or scalogram*, of the absolute values $|(W_\psi f)(b,a)|$ or the real part of $(W_\psi f)(b,a)$. Since the frequency ξ is inversely proportional to the scale a, the time-scale plane (scaleogram) can be regarded as the time-frequency plane by flipping upside down.

The bottom-left is the scaleogram $|(W_\psi f)(b,a)|$ using Meyer wavelet ψ_M. The top-right and the bottom-right are the scaleograms $|(W_\psi f)(b,a)|$ using Dubechies 3 wavelet ψ_{D3} and Mexican hat wavelet ψ_{MH}, respectively. We can detect the position of the cusp from each scaleogram, but these three scaleograms look different. Therefore, we should choose a proper wavelet function for our purpose.

When we compare these three scaleograms, we have a problem. The time-frequency windows of these three wavelets are different both in position and in shape. By the following lemma, we can align the centers of time-frequency windows by translation and dilation (see Figure 3).

Lemma 4.1. *Assume that both w and its Fourier transform $\widehat{w}$ are window functions. Denote by x^* and Δ_w the center and the width of w, and by ξ^* and $\Delta_{\widehat{w}}$ the center and the width of $\widehat{w}$, respectively. Then,*

(i) *$\mathcal{M}_\omega \mathcal{T}_b w$ and $\mathcal{T}_b \mathcal{M}_\omega w$, and their Fourier transforms are window functions, and the time-frequency windows of $\mathcal{M}_\omega \mathcal{T}_b w$ and $\mathcal{T}_b \mathcal{M}_\omega w$ are the same*

$$[x^* + b - \Delta_w, x^* + b + \Delta_w] \times [\xi^* + \omega - \Delta_{\widehat{w}}\,, \xi^* + \omega + \Delta_{\widehat{w}}\,],$$

which is illustrated in Figure 4 (left).

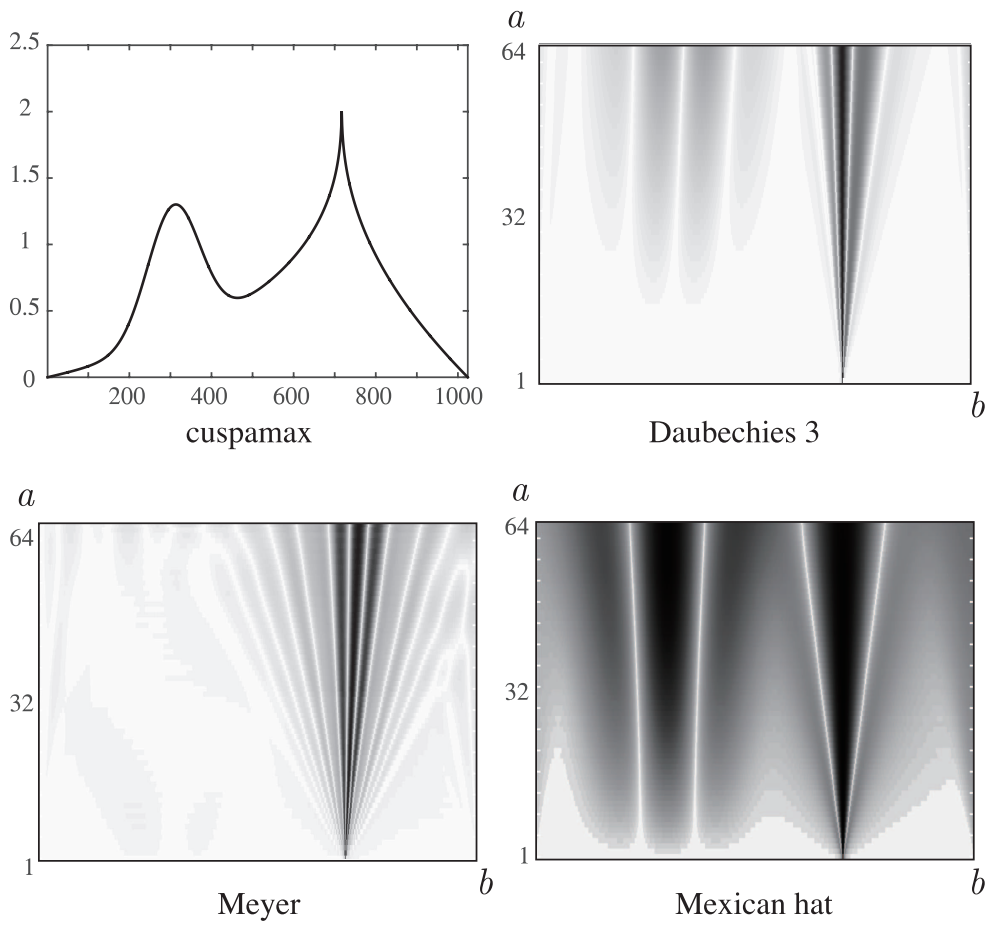

Figure 2. The data cuspamax and its scaleograms.

(ii) *$\mathcal{D}_a w$ and its Fourier transform are window functions, and the time-frequency window of $\mathcal{D}_a w$ is*

$$[ax^* - a\Delta_w, ax^* + a\Delta_w] \times [\xi^*/a - \Delta_{\widehat{w}}/a\,, \xi^*/a + \Delta_{\widehat{w}}/a\,],$$

which is illustrated in Figure 4 (right).

Lemma 4.2. *Let $\psi(x)$ be a wavelet function of one variable $x \in \mathbb{R}$ and $(x^*, \xi^*) \in \mathbb{R}^2$ be the center of ψ with $\xi^* \neq 0$. For a given $(x_0, \xi_0) \in \mathbb{R}^2$ with $\xi_0 \neq 0$, put*

$$b_0 = x_0 - x^*\xi^*/\xi_0, \quad a_0 = \xi^*/\xi_0. \tag{4.1}$$

Then, the center of $\mathcal{T}_{b_0}\mathcal{D}_{a_0}\psi$ is (x_0, ξ_0).

Proof. By Lemma 4.1, the time-frequency window of $\mathcal{M}_0\mathcal{T}_b\mathcal{D}_a w$ is

$$[ax^* + b - a\Delta_w, ax^* + b + a\Delta_w] \times [\xi^*/a - \Delta_{\widehat{w}}/a\,, \xi^*/a + \Delta_{\widehat{w}}/a\,],$$

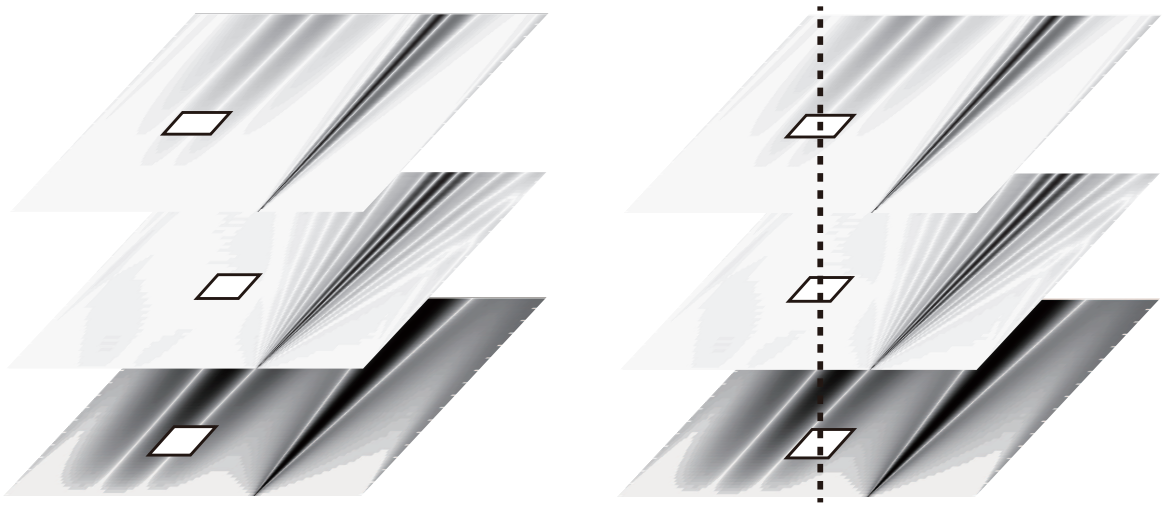

Figure 3. The time-frequency window (left) and the center aligned time-frequency windows (right) of the three wavelets.

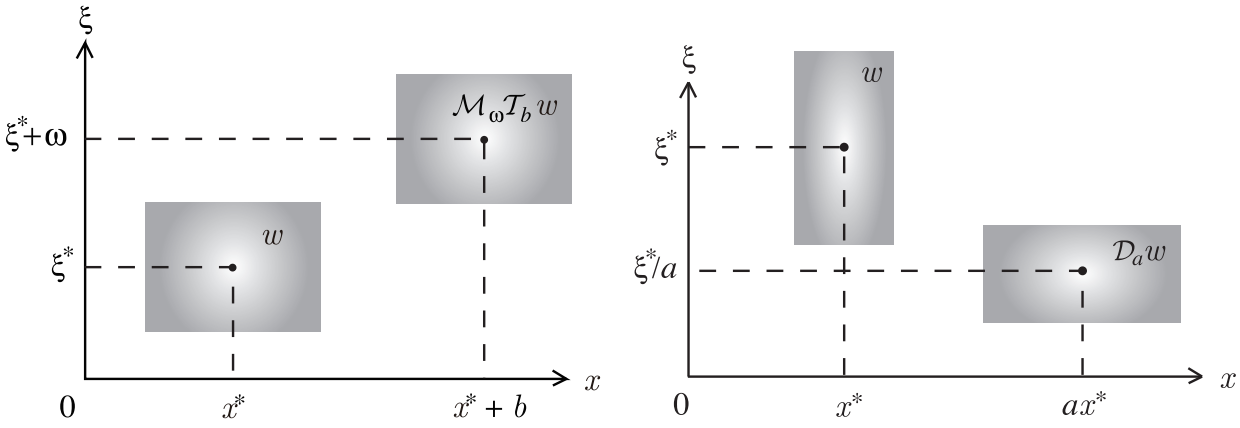

Figure 4. The time-frequency windows of w, $\mathcal{M}_\omega\mathcal{T}_b w$, $\mathcal{D}_a w$.

the center of which is $(ax^* + b, \xi^*/a)$. Solving $(ax^* + b, \xi^*/a) = (x_0, \xi_0)$ with respect to (b, a), we have (4.1). □

Our aim is to align centers of time-frequency windows of several wavelet functions. Let us fix the center $(x_0, \xi_0) \in \mathbb{R}^2$ with $\xi_0 \neq 0$. For every wavelet function ψ of one variable $x \in \mathbb{R}$ and $(x^*, \xi^*) \in \mathbb{R}^2$ with $\xi^* \neq 0$, $\mathcal{T}_{b_0}\mathcal{D}_{a_0}\psi$ is a wavelet function with the center $(x_0, \xi_0) \in \mathbb{R}^2$. As far as the scale parameter a remains to be one dimensional, direct generalization to the multi-dimensional case is difficult except the tensor product of one-dimensional wavelet functions.

Remark. By Lemma 1.3, the continuous wavelet transform $(W_{\mathcal{T}_{b_0}\mathcal{D}_{a_0}\psi} f)(b, a)$

with respect to $\mathcal{T}_{b_0}\mathcal{D}_{a_0}\psi$ can be represented as

$$\begin{aligned}(W_{\mathcal{T}_{b_0}\mathcal{D}_{a_0}\psi}f)(b,a) &= (f, \mathcal{T}_b\mathcal{D}_a\mathcal{T}_{b_0}\mathcal{D}_{a_0}\psi)\\ &= (f, \mathcal{T}_{ab_0+b}\mathcal{D}_{aa_0}\psi) = (W_\psi f)(ab_0+b, aa_0),\end{aligned}$$

which can be calculated by existing continuous wavelet transform programs for $(W_\psi f)(b,a)$, such as the wavelet toolbox in MATLAB.

§ 5. Continuous multiwavelet transform

In this section, we present essentials of the continuous multiwavelet transform according to [3, §5] without proofs. We omit the design of multi-dimensional multiwavelets, which is given in [3, §4].

In practical applications, one of the main difficulties to perform such wavelet analysis with several wavelet functions ψ^p, $p = 1, \dots, P$ is their choice. Since localization of $\mathcal{T}_b\mathcal{D}_a\psi^p$ in the time space and localization of its Fourier transform $\mathcal{F}(\mathcal{T}_b\mathcal{D}_a\psi^p)$ in the frequency space are different in general, we need to choose a space-scale parameter (b,a) properly to access to information at a given time-frequency point.

Definition 5.1. The *continuous multiwavelet transform* of $f \in L^2(\mathbb{R}^n)$ with respect to a multiwavelet function $\Psi = (\psi^p)_{p=1}^P \in L^2(\mathbb{R}^n)^P$, which is considered to be a column vector, is defined by

$$(W_\Psi f)(b,a) := \Big((W_{\psi^p}f)(b,a)\Big)_{p=1}^P, \quad a \in \mathbb{R}_+,\ b \in \mathbb{R}^n.$$

For an essentially bounded function $m \in L^\infty(\mathbb{R}^n)$ called *multiplier* or *mask*, define a *Fourier multiplier operator* $m(D)$ as a bounded linear operator on $L^2(\mathbb{R}^n)$ such that

$$(m(D)f)(x) = \mathcal{F}^{-1}\big(m(\xi)\widehat{f}(\xi)\big), \qquad f \in L^2(\mathbb{R}^n).$$

Here,

$$D = (D_1, \dots, D_n), \qquad D_j = -i\partial/\partial x_j.$$

The continuous wavelet transform has strong compatibility with Fourier multiplier operators defined by homogeneous multipliers. For $m \in L^\infty(\mathbb{R}^n)$, we define $m(D)(\psi^p)_{p=1}^P := (m(D)\psi^p)_{p=1}^P$.

Proposition 5.2 ([3], PROPOSITION 3)**.** *Let $m \in L^\infty(\mathbb{R}^n)$ be positively homogeneous of degree 0, that is, $m(a\xi) = m(\xi)$ for $a \in \mathbb{R}_+$. Then, for $\Psi \in L^2(\mathbb{R}^n)^P$, we have*

$$m(D)W_\Psi f = W_\Psi m(D)f = W_{\overline{m}(D)\Psi}f.$$

Here, $m(D)W_\Psi f$ means $m(D)\big((W_\Psi f)(\cdot,a)\big)$, that is, $m(D)$ acts on the function $W_\Psi f(x,a)$ of x for each fixed $a \in \mathbb{R}_+$.

We give an extended version with two multiwavelet functions Ψ_1 and Ψ_2 like in [7, Chapt.10], although we will use the case when $\Psi_1 = \Psi_2$.

Suppose that $\Psi_1, \Psi_2 \in L^2(\mathbb{R}^n)^P$ satisfy the following condition:

$$(A_{\Psi_1,\Psi_2}) \qquad \begin{array}{c}\text{there exists a constant } M \text{ independent of } \xi \text{ such that}\\ \displaystyle\int_{\mathbb{R}_+} |\widehat{\Psi_1}(a\xi)^* \widehat{\Psi_2}(a\xi)| \,\frac{da}{a} \le M\ , \quad \text{a.e. } \xi \in \mathbb{R}^n \setminus \{0\}.\end{array}$$

We define

$$C_{\Psi_1,\Psi_2}(\xi) := \int_{\mathbb{R}_+} \widehat{\Psi_1}(a\xi)^* \widehat{\Psi_2}(a\xi)\,\frac{da}{a}, \tag{5.1}$$

where $F^* := \overline{F^{\mathrm{T}}}$ is the complex conjugate of the transpose of a vector $F \in \mathbb{C}^P$, and G^*F is the inner product of $F, G \in \mathbb{C}^P$. Since $C_{\Psi_1,\Psi_2}(\xi)$ is positively homogeneous of degree 0, $C_{\Psi_1,\Psi_2} \in L^\infty(\mathbb{R}^n)$. We abbreviate the condition $(A_{\Psi,\Psi})$ as (A_Ψ) and also $C_\Psi(\xi) = C_{\Psi,\Psi}(\xi)$ if Ψ satisfies (A_Ψ). Note that if Ψ_1 and Ψ_2 satisfy (A_{Ψ_1}) and (A_{Ψ_2}), then they satisfy (A_{Ψ_1,Ψ_2}).

A multiwavelet function $\Psi \in L^2(\mathbb{R}^n)^P$ is called an *analyzing multiwavelet* if

$$\Psi \text{ satisfies } (A_\Psi) \text{ and } C_\Psi(\xi) \text{ is a nonzero constant independent of } \xi. \tag{5.2}$$

The condition (5.2) is called the *admissibility condition.*

The *Riesz transforms*, denoted by $\mathcal{R}_j$, $j = 1, \dots, n$, are the Fourier multiplier operators $-i\,D_j/|D|$, that is,

$$\mathcal{R}_j f(x) = \mathcal{F}^{-1}\left(-i\,\frac{\xi_j}{|\xi|}\,\widehat{f}(\xi)\right).$$

The Riesz transforms $\mathcal{R}_j f$, $j = 1, \dots, n$ of real-valued function f are also real-valued.

Define the reflection operator $\mathcal{I}$ by $\mathcal{I}f(x) = f(-x)$. It is easy to see the following Lemma 5.3.

Lemma 5.3 ([3], LEMMA 4)**.** *Let a multiwavelet function Ψ satisfies the admissibility condition.*

(i) *Each of the two multiwavelet functions $(\mathcal{R}_1\Psi; \dots; \mathcal{R}_n\Psi)$ and $(\Psi; \mathcal{R}_1\Psi; \dots; \mathcal{R}_n\Psi)$ also satisfies the admissibility condition, where we use the conventional notation of a semicolon to represent the termination of each row, that is, $(F_1; \dots; F_m) = (F_1^{\mathrm{T}}, \dots, F_m^{\mathrm{T}})^{\mathrm{T}}$.*

(ii) *If $\operatorname{supp}\widehat{\psi^p} \cap \operatorname{supp}\mathcal{I}\widehat{\psi^p} = \emptyset$ for each p, then each of the three multiwavelet functions $\Re\Psi$, $\Im\Psi$, and $(\Re\Psi; \Im\Psi)$ also satisfies the admissibility condition. Here, $\Re$ and $\Im$ denote the real and the imaginary parts, respectively.*

We have the following orthogonality relation and inversion formula for the multiwavelet transform.

Theorem 5.4 ([3], THEOREM 5). (i) *If $\Psi_1, \Psi_2 \in L^2(\mathbb{R}^n)^P$ satisfy (A_{Ψ_1,Ψ_2}), then for $f, g \in L^2(\mathbb{R}^n)$, we have*

$$\langle C_{\Psi_1,\Psi_2}(D)f, g\rangle = \int_{\mathbb{R}_+} \left(\int_{\mathbb{R}^n} (W_{\Psi_2} g)(b,a)^* (W_{\Psi_1} f)(b,a)\, db \right) \frac{da}{a^{n+1}}. \tag{5.3}$$

(ii) *If $\Psi \in L^2(\mathbb{R}^n)^P$ satisfies (A_Ψ), then W_Ψ is a bounded linear operator from $L^2(\mathbb{R}^n)$ to $L^2(\mathbb{R}^n \times \mathbb{R}_+, dbda/a^{n+1})^P$.*

(iii) *If $\Psi_1, \Psi_2 \in L^2(\mathbb{R}^n)^P$ satisfy (A_{Ψ_1,Ψ_2}) and C_{Ψ_1,Ψ_2} is a nonzero constant independent of ξ, then any function $f \in L^2(\mathbb{R}^n)$ is reconstructed from its multiwavelet transform by*

$$f = \frac{1}{C_{\Psi_1,\Psi_2}} \int_{\mathbb{R}^n \times \mathbb{R}_+} (\mathcal{T}_b \mathcal{D}_a \Psi_2)^{\mathrm{T}} (W_{\Psi_1} f)(b,a)\, \frac{db\, da}{a^{n+1}}. \tag{5.4}$$

Especially, if Ψ is an analysing multiwavelet, then we have the inversion formula

$$f = \frac{1}{C_\Psi} \int_{\mathbb{R}^n \times \mathbb{R}_+} (\mathcal{T}_b \mathcal{D}_a \Psi)^{\mathrm{T}} (W_\Psi f)(b,a)\, \frac{db\, da}{a^{n+1}}. \tag{5.5}$$

The right-hand side of the above inversion formula

$$W_\Psi^{-1} F := \frac{1}{C_\Psi} \int_{\mathbb{R}^n \times \mathbb{R}_+} (\mathcal{T}_b \mathcal{D}_a \Psi)^{\mathrm{T}} F(b,a)\, \frac{db\, da}{a^{n+1}} \in L^2(\mathbb{R}^n) \tag{5.6}$$

is called the *inverse multiwavelet transform* of $F \in L^2(\mathbb{R}^n \times \mathbb{R}_+, dbda/a^{n+1})^P$. The integrals in (5.4)–(5.6) are interpreted in the weak sense as in [7, Corollary 10.3].

For the discrete multiwavelet, for example see [11, §7.1], the scaling functions are important. In most cases, there are several scaling functions, each corresponds to $(2^n - 1)$ wavelet functions. On the other hand, in [12, §4.3]C Mallat considered a scaling function for continuous wavelet transform, which aggregates the part of large a. We can also consider a *multiscaling function* Φ as follows.

Theorem 5.5 ([3], THEOREM 7). *Suppose that $\Psi_1, \Psi_2 \in L^2(\mathbb{R}^n)^P$ and $\Phi_1, \Phi_2 \in L^2(\mathbb{R}^n)^Q$. Also suppose that there exists a constant M such that*

$$\int_0^1 |\widehat{\Psi_1}(a\xi)^* \widehat{\Psi_2}(a\xi)| \frac{da}{a} + |\widehat{\Phi_1}(\xi)^* \widehat{\Phi_2}(\xi)| \le M \quad \text{a.e. } \xi \text{ in } \mathbb{R}^n. \tag{5.7}$$

Set

$$C_{\Psi_1,\Psi_2;\Phi_1,\Phi_2}(\xi) := \int_0^1 \widehat{\Psi_1}(a\xi)^* \widehat{\Psi_2}(a\xi) \frac{da}{a} + \widehat{\Phi_1}(\xi)^* \widehat{\Phi_2}(\xi) \in L^\infty(\mathbb{R}^n). \tag{5.8}$$

Then, we have the following.

(i) *For $f, g \in L^2(\mathbb{R}^n)$ and $a_0 \in \mathbb{R}_+$, we have*

$$\begin{aligned}(5.9)\quad \langle C_{\Psi_1,\Psi_2;\Phi_1,\Phi_2}(a_0 D)f, g\rangle &= \int_0^{a_0} \left(\int_{\mathbb{R}^n} (W_{\Psi_2} g)(b,a)^* (W_{\Psi_1} f)(b,a)\, db \right) \frac{da}{a^{n+1}} \\ &\quad + \frac{1}{a_0^n} \int_{\mathbb{R}^n} (W_{\Phi_2} g)(b,a_0)^* (W_{\Phi_1} f)(b,a_0)\, db.\end{aligned}$$

(ii) *If $C_{\Psi_1,\Psi_2;\Phi_1,\Phi_2}$ is a nonzero constant, then any function $f \in L^2(\mathbb{R}^n)$ is reconstructed by*

$$\begin{aligned}(5.10)\quad f = \frac{1}{C_{\Psi_1,\Psi_2;\Phi_1,\Phi_2}} \Bigg\{ &\int_{\mathbb{R}^n \times (0,a_0)} (\mathcal{T}_b \mathcal{D}_a \Psi_2)^{\mathrm{T}} (W_{\Psi_1} f)(b,a) \frac{db\, da}{a^{n+1}} \\ &+ \frac{1}{a_0^n} \int_{\mathbb{R}^n} (\mathcal{T}_b \mathcal{D}_{a_0} \Phi_2)^{\mathrm{T}} (W_{\Phi_1} f)(b,a_0)\, db \Bigg\}.\end{aligned}$$

Remark. Assume that C_{Ψ_1,Ψ_2} is a constant. If $\Phi_1, \Phi_2 \in L^2(\mathbb{R}^n)^Q$ satisfies

$$\widehat{\Phi_1}(\xi)^* \widehat{\Phi_2}(\xi) = \int_1^\infty \widehat{\Psi_1}(a\xi)^* \widehat{\Psi_2}(a\xi) \frac{da}{a}, \quad \text{a.e. } \xi \in \mathbb{R}^n,$$

then $C_{\Psi_1,\Psi_2;\Phi_1,\Phi_2}(\xi) = C_{\Psi_1,\Psi_2}$ a.e. This enables us to construct Φ's from Ψ's.

§ 6. Blind signal separation

Assume several persons are talking in a cocktail party. One can focus one's auditory attention on a particular person and understand his or her talk. How one's auditory perception works? This is what we call *cocktail party problem*. One of basic questions for the cocktail party problem is how to build a machine to solve the cocktail party problem in a satisfactory manner. This question corresponds to *blind signal separation* or *blind source separation* (BSS) [8]. The purpose of blind signal separation is to separate and to estimate the original sources (talks by N persons, N is unknown) from the observed signals (recorded talks with M microphones, M is known) as in Figure 5. To estimate the number N of sources is one of the most difficult procedures in the blind signal separation. As the blind signal separation is a inverse problem, certain *a priori* knowledge on the original sources is needed for this separation, and the original sources cannot be uniquely estimated. Besides methods based on independent component analysis [9] which is one of the most powerful tools for blind signal separation, several methods based on time-frequency analysis have been proposed. One of them is the quotient signal estimation method which can estimate the unknown number of sources [6, 10, 13, 14].

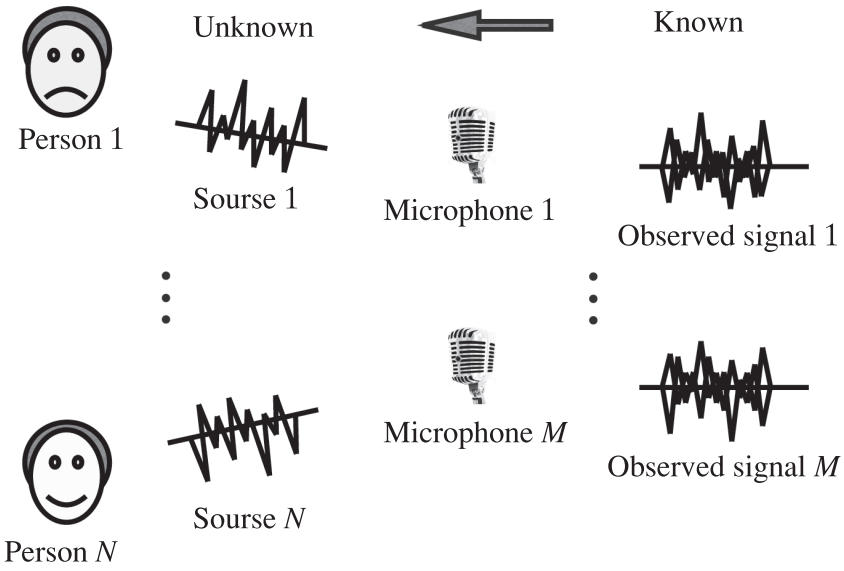

Figure 5. Blind signal separation.

We explain the blind signal separation of one-dimensional signals based on [1, 2, 4]. Let $\{s_k(t)\}_{k=1}^N$ be the original source signals and $\{x_j(t)\}_{j=1}^M$ be the observed signals. Assume that $M \geq N$ and all of these signals are real-valued. Put

$$s(t) = (s_1(t), \dots, s_N(t))^T, \qquad x(t) = (x_1(t), \dots, x_M(t))^T.$$

The *spatial mixture problem* of BSS assumes that the observed signals $\{x_j(t)\}_{j=1}^M$ can be represented as

$$x_j(t) = \sum_{k=1}^N a_{j,k} s_k(t), \qquad a_{j,k} \in \mathbb{R}, \tag{6.1}$$

for unknown matrix $A = (a_{j,k}) \in \mathbb{R}^{M\times N}$, which is called *mixing matrix*. Here, $\mathbb{R}^{M\times N}$ denotes the set of $M \times N$ matrices with real elements. We assume $a_{j,k} \in \mathbb{R}_+$, for the sake of simplicity.

Assume we know the number N and the set of points $\{t_\ell\}_{\ell=1}^N$ such that $s_k(t_\ell) = \delta_{k,\ell}$, for $\ell, k = 1, \dots, N$. Here $\delta_{k,\ell}$ denotes the Kronecker delta. Then, (6.1) implies

$$x_j(t_\ell) = \sum_{k=1}^N a_{j,k} s_k(t_\ell) = \sum_{k=1}^N a_{j,k}\delta_{k,\ell} = a_{j,\ell}, \tag{6.2}$$

which gives us an estimation of $A = (x_j(t_\ell))$. Applying the Fourier transform to (6.1), we have

$$\widehat{x}_j(\omega) = \sum_{k=1}^N a_{j,k}\widehat{s}_k(\omega). \tag{6.3}$$

Again, assume we know the number N and the set of points $\{\omega_\ell\}_{\ell=1}^N$ such that $\widehat{s}_k(\omega_\ell) = \delta_{k,\ell}$, for $\ell, k = 1, \ldots, N$. Then, we have

$$\widehat{x}_j(\omega_\ell) = \sum_{k=1}^{N} a_{j,k}\widehat{s}_k(\omega_\ell) = \sum_{k=1}^{N} a_{j,k}\delta_{k,\ell} = a_{j,\ell}, \tag{6.4}$$

which gives us another estimation of $A = (\widehat{x}_j(\omega_\ell))$. Which is easy to find such set of points, $\{t_\ell\}_{\ell=1}^N$ or $\{\omega_\ell\}_{\ell=1}^N$? If one person is talking all the time, it is impossible to find $\{t_\ell\}_{\ell=1}^N$. Even such a situation, if their voices are different in frequency, it may be possible to find $\{\omega_\ell\}_{\ell=1}^N$. Moreover, if we use time-frequency information, finding a set of points $\{(t_\ell, \omega_\ell)\}_{\ell=1}^N$ should be better. In Figure 6, the original sources are

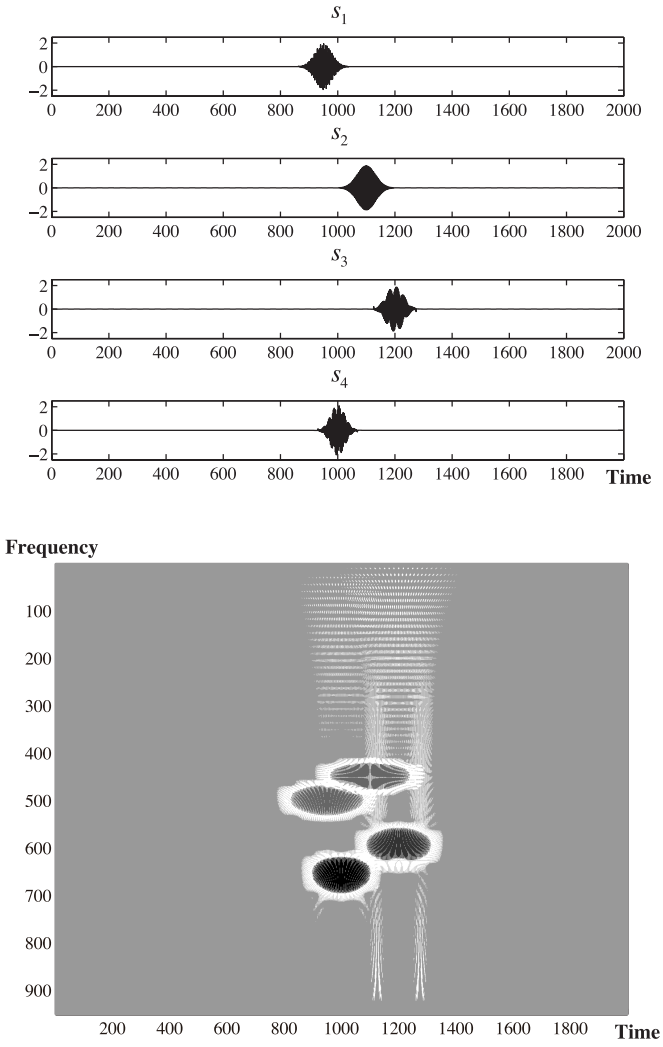

Figure 6. Original sources (top) and their time-frequency information (bottom).

shown in the top and their continuous wavelet transforms are bottom, where the scale

is transformed to frequency using the fact that $1/a$ is in proportion to frequency ω. Only one transformed source signal is not zero on each oval region, more than one transformed source signals are not zero on the white region, all the transformed source signals are zero on the gray region. The overlapping of transformed source signals (bottom) in the time-frequency region are rather small comparing to the overlapping of original source signals (top) in the time region.

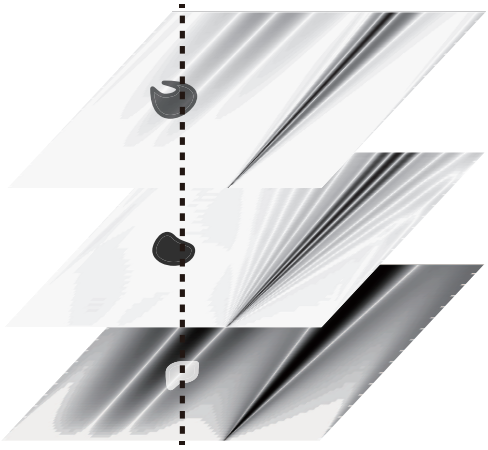

Figure 7. Intersection of candidates given by all the continuous wavelet transforms.

Let ψ^p, $p = 1, \ldots, L$ be real wavelet functions. Define the time-frequency information of s_k and x_j with respect to the wavelet function ψ^p by

$$\begin{aligned} S_k^p(t,\omega) &= W_{\psi^p} s_k(t, c_{\widehat{\psi^p},1}/\omega), \\ X_j^p(t,\omega) &= W_{\psi^p} x_j(t, c_{\widehat{\psi^p},1}/\omega), \qquad \omega \in \mathbb{R}_+, \end{aligned}$$

where $c_{\widehat{\psi^p},1}$ is the center of $\widehat{\psi^p}$. Note that the continuous wavelet transform of (6.1) with respect to ψ^p is

$$X_j^p(t,\omega) = \sum_{k=1}^{N} a_{j,k}\, S_k^p(t,\omega). \tag{6.5}$$

Each continuous wavelet transform of (6.1) with respect to ψ^p gives candidates for such set of points. We anticipate that the intersection of candidates chosen by all the continuous wavelet transforms gives more precise estimation. Figure 7 illustrates this idea (the data are not real ones). In fact, the intersection makes our estimations of N and A more precise. The details can be found in [5, §3].

In [2, 3] and [3, §6], we proposed a source signal estimation method which can estimate all the elements of the mixing matrix at once. These estimation methods have a difficulty when several clusters are quite crowded comparing to others. To overcome

this difficulty, we propose use informations of several continuous wavelet transforms, which we call the continuous multiwavelet transform. In estimating the number N of sources and sources images s_j, $j = 1, \ldots, N$, the performance of this new method is substantially improved.

§ 7. Image separation

Let us present a numerical experiment for image separation. In this simulation, we use the annular sector multiwavelets given in [3, §4] for time-scale informations.

Note that the time-frequency windows of multiwavelets $\Re\psi_p$ and $\Im\psi_p$ are the same for each p. Density plots of annular sector multiwavelets $\Re\psi_p$ and $\Im\psi_p$ are shown in the right column of Figure 8.

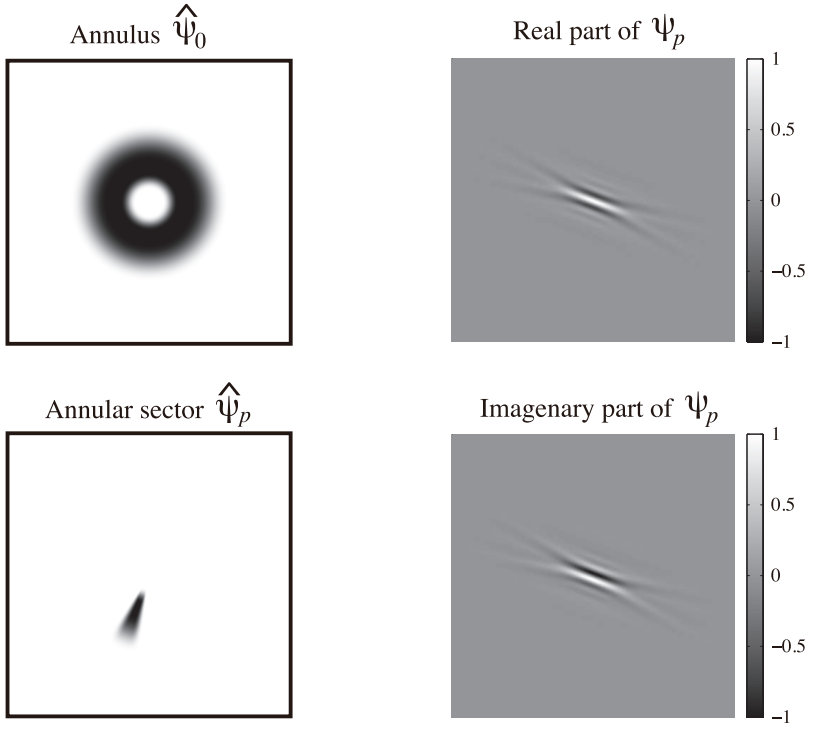

Figure 8. Annular sector multiwavelets.

The mixing matrix $A \in \mathbb{R}^{3\times 3}$ is a random matrix uniformly distributed in $[0.2, 0.8]$ as follows:

$$A = \begin{pmatrix} 0.2091 & 0.3515 & 0.3481 \\ 0.2410 & 0.2888 & 0.7472 \\ 0.4841 & 0.2637 & 0.6455 \end{pmatrix}.$$

Since the condition number of A is $\mathrm{cond}(A) = 7.0203$, it implies that A is a good matrix for inversion. Three 512×512 standard gray scale images: Lena, Peppers, Stream

and bridge are used as the original source images s_1, s_2, s_3 shown in the first row of Figure 9. Three mixed images x_1, x_2, x_3 shown in the second row of Figure 9 are produced by (6.1) with the above mixing matrix A. By applying the source reduction method proposed in [5, §4], we have our estimated images shown in the third row of Figure 9. The ordering of estimation images is unavoidable ambiguity. The correct ordering should be $(s_1, s_2, s_3) \longleftrightarrow (\sigma_2, \sigma_1, \sigma_3)$. The performance of our estimation σ_1,

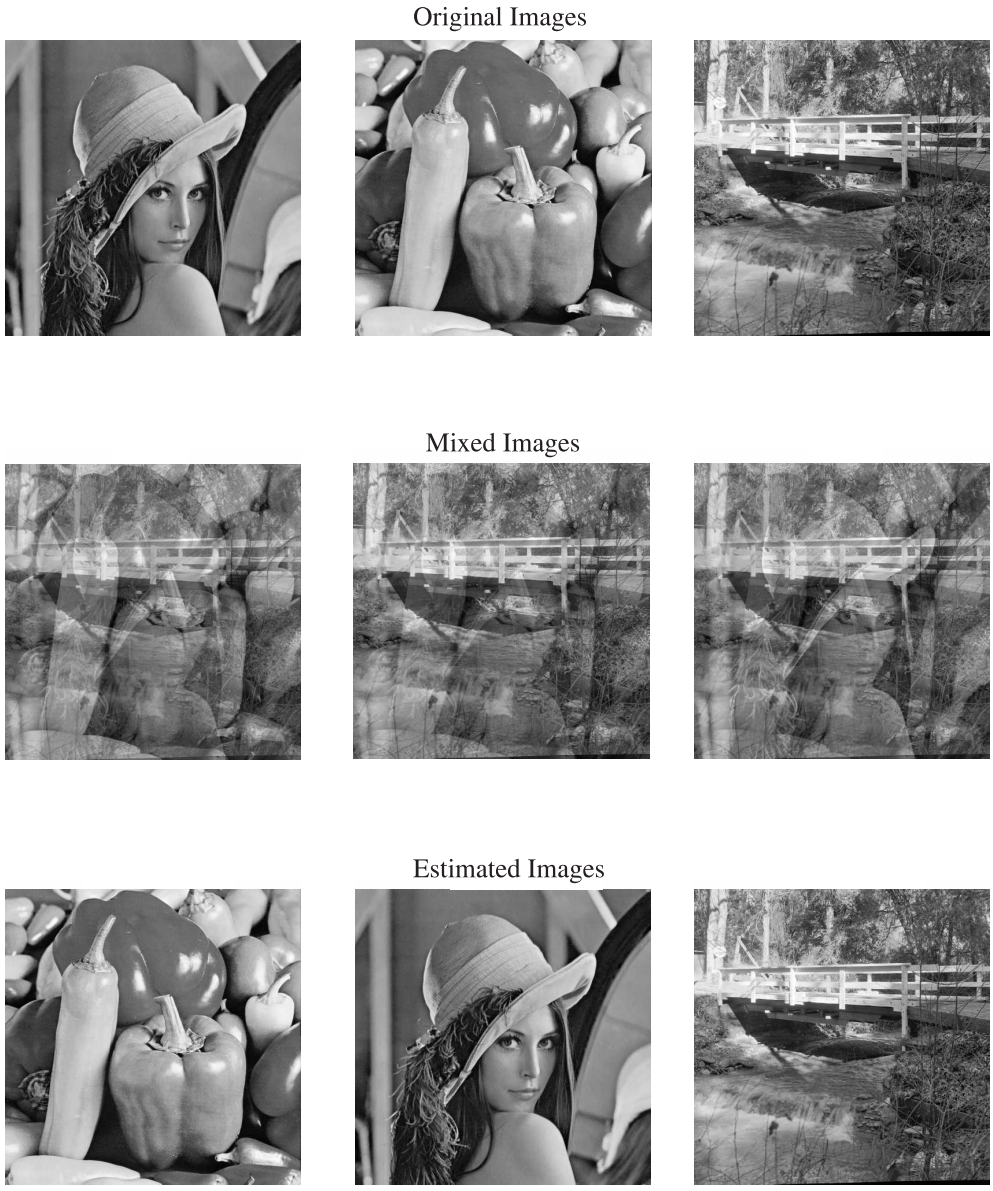

Figure 9. Image separation.

σ_2, σ_3 are very accurate as shown in Table 1.

Table 1. Various errors of the estimation.

Original	Estimated	max error [%]	ℓ^1-error [%]	ℓ^2-error [%]	SNR [dB]
s_1	σ_2	0.48216	0.4821	0.48506	46.284
s_2	σ_1	0.60761	0.64921	0.46612	46.63
s_3	σ_3	1.5549	1.9087	1.9886	34.0293

§ 8. Acknowledgements

The author would like to thank the anonymous referees for their valuable comments and useful suggestions to improve this paper.

References

[1] R. Ashino, C. A. Berenstein, K. Fujita, A. Morimoto, M. Morimoto, D. Napoletani, and Y. Takei, Mathematical background for a method on quotient signal decomposition,

[2] R. Ashino, K. Fujita, T. Mandai, A. Morimoto, and K. Nishihara, Blind source separation using time-frequency information matrix given by several wavelet transforms, *Information*, **10** (5), 555–568, 2007.

[3] R. Ashino, S. Kataoka, T. Mandai and A. Morimoto, Blind image source separations by wavelet analysis, *Appli. Anal.*, **91** (4), 617–644, 2012.

[4] R. Ashino, T. Mandai, A. Morimoto, and F. Sasaki, Blind source separation of spatio-temporal mixed signals using time-frequency analysis, *Appli. Anal.*, **88** (3), 425–456, 2009.

[5] R. Ashino, T. Mandai and A. Morimoto, Multistage blind source separations by wavelet analysis, *Int. J. Wavelets Multiresolut. Inf. Process.*, **12** (4), 1460004, 25, 2014.

[6] R. Balan and J. Rosca, Statistical properties of STFT ratios for two channel systems and applications to blind source separation, in *Proceedings of the 2nd International Workshop on Independent Component Analysis and Blind Signal Separation, Helsinki, Finland, June 2000*, 19–22.

[7] K. Gröchenig, *Foundations of Time-frequency Analysis*, Birkhäuser Boston, Inc., Boston, MA, 2001.

[8] S. Haykin and Z. Chen, The cocktail party problem, *Neural Computation*, **17** (9), 1875–1902, 2005.

[9] A. Hyvärinen, J. Karhunen, E. Oja, *Independent Component Analysis*, John Wiley & Sons, New York, NY, 2001.

[10] A. Jourjine, S. Rickard, and O. Yilmaz, Blind separation of disjoint orthogonal signals: Demixing N sources from 2 mixtures, in *Proceedings of the 2000 IEEE International Conference on Acoustics, Speech, and Signal Processing*, **5**, 2985–2988, 2000.

[11] F. Keinert, *Wavelets and Multiwavelets*, Studies in Advanced Mathematics, Chapman & Hall/CRC, 2004.

[12] S. MALLAT, *A Wavelet Tour of Signal Processing — The Sparse Way*, Third Edition, Academic Press, 2009.

[13] D. NAPOLETANI, C. A. BERENSTEIN, P. S. KRISHNAPRASAD, AND D. C. STRUPPA, Quotient signal estimation, in *Harminic Analysis, Signal Processing, and Complexity*, Progr. Math., **238**, Birkhäuser, Boston, MA, 2005, 151–162.

[14] O. YILMAZ AND S. RICKARD, Blind source separation of speech mixtures via time-frequency masking, *IEEE Transactions on Signal Processing*, **52**, 1830–1847, 2004.